

Defining the Interaction of Human Soluble Lectin ZG16p and Mycobacterial Phosphatidylinositol Mannosides

Shinya Hanashima,^[a] Sebastian Götze,^[b, c] Yan Liu,^[d] Akemi Ikeda,^[a] Kyoko Kojima-Aikawa,^[e] Naoyuki Taniguchi,^[f] Daniel Varón Silva,^[b, c] Ten Feizi,^[d] Peter H. Seeberger,^[b, c] and Yoshiki Yamaguchi^{*[a]}

ZG16p is a soluble mammalian lectin that interacts with mannose and heparan sulfate. Here we describe detailed analysis of the interaction of human ZG16p with mycobacterial phosphatidylinositol mannosides (PIMs) by glycan microarray and NMR. Pathogen-related glycan microarray analysis identified phosphatidylinositol mono- and di-mannosides (PIM1 and PIM2) as novel ligand candidates of ZG16p. Saturation transfer difference (STD) NMR and transferred NOE experiments with

chemically synthesized PIM glycans indicate that PIMs preferentially interact with ZG16p by using the mannose residues. The binding site of PIM was identified by chemical-shift perturbation experiments with uniformly ¹⁵N-labeled ZG16p. NMR results with docking simulations suggest a binding mode of ZG16p and PIM glycan; this will help to elucidate the physiological role of ZG16p.

Introduction

ZG16p is a soluble protein that was initially identified in rat pancreas where it is associated with the zymogen granule membrane.^[1] The protein was recently detected in human colon, small intestine, and serum, as well as in the pancreas.^[2] ZG16p plays a role in packaging pancreatic enzymes into zymogen granules and separating them from constitutively secreted proteins.^[3] ZG16p has been proposed as a primary binding partner of glycosaminoglycans (GAGs) in pancreatic granules.^[4]

The ZG16p amino acid sequence has homology with the carbohydrate-recognition domain (CRD) of jacalin, a jackfruit lectin.^[4–5] A recent X-ray crystallographic analysis revealed that human ZG16p has a jacalin-related β -prism fold, similar to that in Banlec, a mannose-binding lectin in bananas.^[5] Glycan microarray screening has demonstrated that ZG16p has specificity for glycans consisting of mannose, including mannan and Ser/Thr-linked O-mannose.^[2,5–6] Asp151 is a key mannose-binding residue, as mutation of Asp151 to Asn abolished glycan binding.^[2] Interestingly, ZG16p also binds GAGs, especially heparin and heparan sulfate.^[4] Our recent crystallographic and NMR studies indicated that mannose and GAG binding to ZG16p occurs with distinct binding modes:^[6] mannose uses a shallow binding site made from three loops (the GG loop (between β 1 and β 2 strands, Gly31–Gly35), the recognition loop (between β 7 and β 8, Lys102–Tyr104), and the binding loop (between β 11 and β 12, Ser146–Leu149)), whereas sulfated oligosaccharides bind to a positively charged surface consisting of a cluster of basic amino acid residues.

Most of the mannose-binding animal C-type lectins, including dendritic cell-specific intercellular adhesion molecule-3-grabbing non-integrin (DC-SIGN), the mannose receptor, Dectin-2, macrophage inducible C-type lectin (Mincle), and Langerin, are involved in host immunity through recognition of the mannans of pathogenic bacteria.^[7]

Most of these lectins are signaling molecules with transmembrane domains, although some, also involved in host immunity, are secreted. Mannose-binding lectin (MBL) is a liver-derived serum protein that has a role in the innate immune response by binding to the surface glycans of a wide range of pathogens.^[7a,11] Proteins of the regenerating islet-derived (Reg) family are secreted proteins containing a C-type lectin-like

[a] Dr. S. Hanashima,⁺ A. Ikeda, Dr. Y. Yamaguchi
Structural Glycobiology Team
RIKEN-Max Planck Joint Research Center for Systems Chemical Biology
RIKEN Global Research Cluster
Wako, Saitama 351-0198 (Japan)
E-mail: yyoshiki@riken.jp

[b] Dr. S. Götze,⁺ Dr. D. Varón Silva, Prof. P. H. Seeberger
Department of Biomolecular Systems
Max Planck Institute of Colloids and Interfaces
Am Mühlenberg 1, 14424 Potsdam (Germany)

[c] Dr. S. Götze,⁺ Dr. D. Varón Silva, Prof. P. H. Seeberger
Institute of Chemistry and Biochemistry, Freie Universität Berlin
Arnimallee 22, 14195 Berlin (Germany)

[d] Dr. Y. Liu,⁺ Prof. T. Feizi
Glycosciences Laboratory, Department of Medicine
Imperial College London
Du Cane Road, London W12 0NN (UK)

[e] Prof. K. Kojima-Aikawa
The Glycoscience Institute, Ochanomizu University
Otsuka, Bunkyo-ku, Tokyo 112-8610 (Japan)

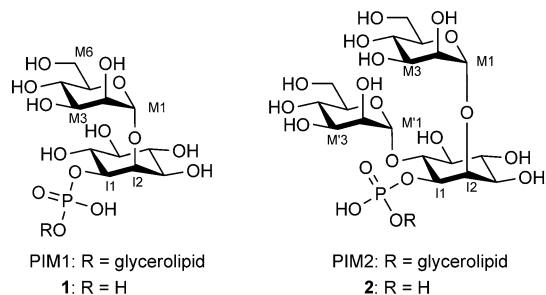
[f] Prof. N. Taniguchi
Disease Glycomics Team
RIKEN-Max Planck Joint Research Center for Systems Chemical Biology
RIKEN Global Research Cluster
Wako, Saitama 351-0198 (Japan)

[⁺] These authors contributed equally to this work.

Supporting information for this article is available on the WWW under <http://dx.doi.org/10.1002/cbic.201500103>.

domain, and play a role in pancreatic function and associated diseases.^[12]

Similar to the C-type lectins and Regs, ZG16p binds pathogenic fungi *Candida* and *Malassezia* in a mannose-dependent manner.^[2] Therefore, it is possible that human ZG16p is involved in the gastrointestinal immune system through binding target glycans of pathogens. In order to gain insights into the structure–function relationships of ZG16p in pathogen recognition, we determined the glycan-binding specificity of ZG16p by using a pathogen-related glycan microarray. ZG16p binds to phosphatidyl inositol mannosides (PIM1 and PIM2, Scheme 1), major cell-wall components of some pathogenic



Scheme 1. Chemical structures of PIM1 and PIM2 and synthesized PIM glycans 1 and 2.

bacteria including *Mycobacterium tuberculosis*.^[16] We also elucidated details of the binding mode of human ZG16p with PIM glycans by using NMR experiments and docking simulations. The findings raise the possibility that human ZG16p is involved in mucosal defense against bacteria through recognitions of short PIM glycans.

Bacterial infections and host defense mechanisms must be studied from various aspects. The huge diversity of bacterial glycans and the presence of numerous uncharacterized host lectins preclude rapid progress in this research area. The binding preference of human ZG16p lectin is unique in that it involves both mannose and sulfated glycosaminoglycans. However the role of ZG16p has not yet been fully characterized in terms of sugar binding. Here we combine glycan array screening, synthetic chemistry and structural biology approaches to elucidate the possible role and mechanism of ZG16p in pathogen recognition.

Results and Discussion

Pathogen glycan-focused microarray

We speculated that ZG16p plays a role in the host immune defense by binding cell-wall glycans of pathogenic bacteria, hence we performed a pathogen-related carbohydrate microarray analysis (Figure 1).^[17] The array (Table 1) comprised a small set of glycoconjugates, lipid-linked glycans, and polysaccharides derived from mycobacteria and fungal pathogens, in addition to mannose-containing mammalian neoglycolipids (Probes 1–4, Table 1) that were tested with ZG16p in a previous

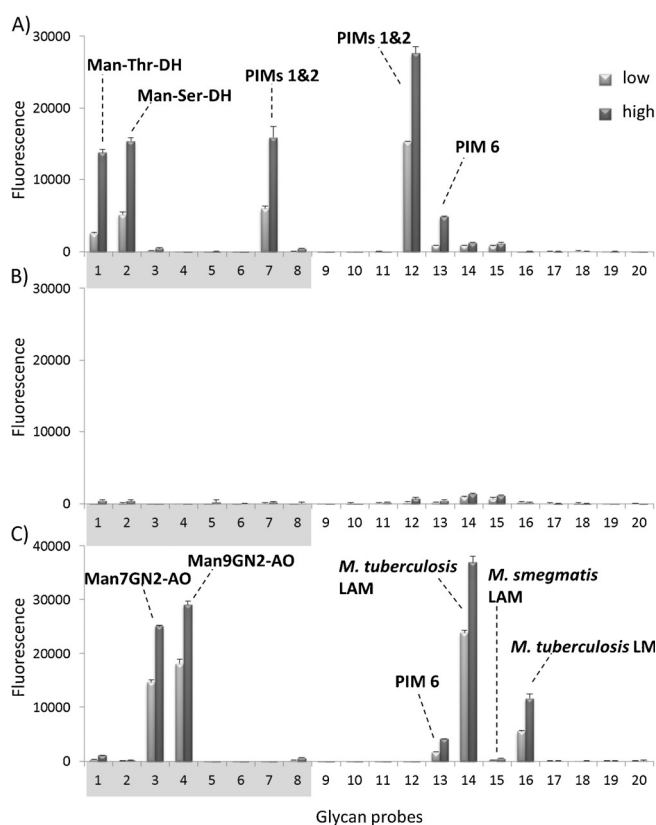


Figure 1. Microarray analysis of a small pathogen-related array of glycan probes (lipid-tagged probes or polysaccharides). The fluorescence intensities are shown for A) wild-type ZG16p, B) the D151N mutant, and C) plant lectin Con A (included for comparison). Glycan probes are detailed in Table 1. Each probe was printed in duplicate at two levels (light and dark gray bars; 1–8: 2 and 5 fmol per spot; 9–20: 0.03 and 0.1 ng).

study^[6] and served as controls here. Wild-type ZG16p gave strong binding signals with PIM1 and PIM2 (arrayed as a mixture), with similar intensities to those for the positive controls 1 and 2 (Man-Thr-DH and Man-Ser-DH; Figure 1 A). Interestingly, the intensity for hexamannoside PIM6 was much lower. PIM2 and PIM6 are the two most abundant PIM classes in *Mycobacterium bovis*, *M. tuberculosis* H37Rv, and *Mycobacterium smegmatis* 607 (Figure S1 in the Supporting Information).^[18] ZG16p preferentially bound PIM1 and PIM2 over PIM6. DC-SIGN, through its interaction with PIMs, is considered a key molecule during infection with *M. tuberculosis*.^[19] In contrast to ZG16p, DC-SIGN preferentially binds PIM5 and PIM6 over shorter PIMs.^[20] In contrast, the D151N mutant of ZG16p^[2] showed little or no bindings to these probes (Figure 1 B), in accordance with a previous report on loss of mannose binding.^[2] Lipoarabinomannan (LAM) and lipomannan (LM), the major glycolipids in the cell wall of all *Mycobacterium* species, elicited little or no binding signal with ZG16p. LAM and LM from *M. tuberculosis* (but not LAM from *M. smegmatis*; capped by phosphatidyl inositols) were well bound by plant lectin concanavalin A (Con A), which was included as a positive control (Figure 1 C). No significant binding was observed for ZG16p to *M. tuberculosis* cord factor trehalose-6,6'-dimycolate (TDM), sulfolipids, or arabinogalactans, nor to the fungal-derived glucan

Table 1. Glycan probes in the microarray analysis.		
No.	Probe ^[a]	Structure
1	Man-Thr-DH	Man α -Thr-DH ^[b]
2	Man-Ser-DH	Man α -Ser-DH
3	Man7(D1)GN2-AO	
4	Man9GN2-AO	
5	<i>M. tuberculosis</i> TDM	purified trehalose dimycolate (TDM) from <i>M. tuberculosis</i> , strain H37Rv (BEI number NR-14844)
6	TDB	trehalose-6,6-dibehenate (TDB), a synthetic analogue of TDM (Sigma)
7	<i>M. tuberculosis</i> PIMs 1 and 2	purified PIM 1 and 2 from <i>M. tuberculosis</i> , strain H37Rv (BEI number NR-14846)
8	<i>M. tuberculosis</i> PIM 6	purified PIM 6 from <i>M. tuberculosis</i> , Strain H37Rv (BEI number NR-14847)
9	<i>M. tuberculosis</i> MME	purified mycolic acid methyl esters from <i>M. tuberculosis</i> , Strain H37Rv (BEI number NR-14854)
10	<i>M. tuberculosis</i> TDM	as for probe 5
11	<i>M. tuberculosis</i> Sulfolipid-1	purified sulfolipid-1 from <i>M. tuberculosis</i> , Strain H37Rv (BEI number NR-14845)
12	<i>M. tuberculosis</i> PIMs 1 and 2	as for probe 7
13	<i>M. tuberculosis</i> PIM 6	as for probe 8
14	<i>M. tuberculosis</i> LAM	purified lipoarabinomannan (LAM) from <i>M. tuberculosis</i> , strain H37Rv (BEI number NR-14848)
15	<i>M. smegmatis</i> LAM	purified LAM from <i>M. smegmatis</i> (BEI number NR-14849)
16	<i>M. tuberculosis</i> LM	purified lipomannan (LM) from <i>M. tuberculosis</i> , strain H37Rv (BEI number NR-14850)
17	<i>M. tuberculosis</i> arabinogalactan	purified arabinogalactan from <i>M. tuberculosis</i> , strain H37Rv (BEI number NR-14852)
18	pullulan from <i>Pullularia pullulans</i>	mixed-linked α 1-4, α 1-6 glucose polysaccharide (Megazyme)
19	curdlan from <i>Alcaligenes faecalis</i>	β 1-3 glucose polysaccharide (in 50 mM NaOH) (Megazyme)
20	pustulan from <i>Umbilicaria papullosa</i>	β 1-6 glucose polysaccharide (CalBiochem)

[a] Probes 1–8 were printed at 2 and 5 fmol per spot; the rest were at 0.03 and 0.1 ng per spot. The neoglycolipids (positions 1–4) are from the collection assembled in the course of research in the Glycosciences Laboratory at Imperial College. [b] DH, amino lipid 1,2-dihexadecyl-*sn*-glycero-3-phosphoethanolamine (DHPE). [c] AO, aminoxy-functionalized DHPE.

polysaccharides. The glycan array data suggest that ZG16p has a preference for short α -mannose-related glycans, including PIM1 and 2, over more-complex mannose-containing glycans.

Chemical synthesis of PIM1 and PIM2 glycans 1 and 2

To investigate the binding mode of ZG16p to PIM1 and PIM2 by NMR, we prepared phosphoglycans **1** and **2** by reported procedures with some modifications (Scheme 2).^[21] Instead of a phosphodiester bearing a diacylglycerol moiety or functionality that enables covalent attachment to surfaces or beads, PIM1 glycan **1** and PIM2 glycan **2** structures used in our experiments had a monoester of phosphoric acid at the C1-position of *myo*-inositol to ensure solubility. The syntheses of **1** and **2**

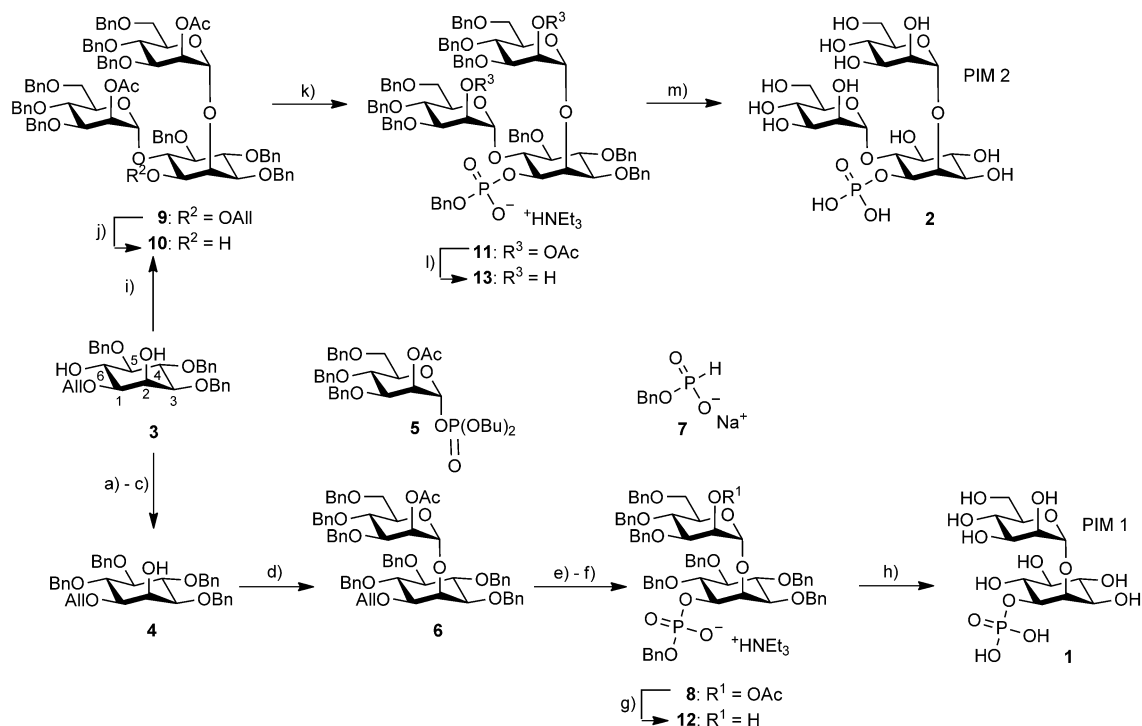
commenced from the *myo*-inositol building block **3**.^[22] To prepare **1**, a temporary *para*-methoxybenzyl (PMB) ether was placed at C2 of **3**, followed by benzylation and acidic cleavage to furnish glycosyl acceptor **4** in 58% yield over three steps. Glycosylation of **4** with phosphate **5**^[23] at -40°C in toluene exclusively formed the α -linked pseudodisaccharide **6** in 84% yield ($^1J_{\text{C1-H1}} = 175\text{ Hz}$). In situ isomerization of the allyl ether generated iridium hydride,^[24] and hydrolysis of the corresponding enol ether resulted in an alcohol function at C1 of inositol. Phosphorylation with the mixed anhydride of pivalic acid and *H*-phosphonate **7**^[25] followed by oxidation provided the triethylammonium salt **8** in 73% yield over three steps from **6**. Subjecting **8** to deacetylation and subsequent final hydrogenolysis over palladium in methanol yielded **1** in excellent yield (97%) over two steps.

The synthesis of **2** continued with double glycosylation of **3** with **5** under conditions similar to those used in the synthesis of **6**. Pseudotrisaccharide **9** was obtained in 62% yield, and the α -configuration of both anomeric linkages was confirmed ($^1J_{\text{C1-H1}} = 173$ and 176 Hz). Exposure of **9** to PdCl_2 in CH_2Cl_2 /methanol selectively removed the allyl ether (64% yield). Final phosphorylation of the corresponding alcohol **10** with **7** formed phosphate

11, which was deacetylated and submitted to hydrogenolysis to provide **2** in 49% yield over four steps.

STD-NMR analysis of the interaction of PIM glycans with ZG16p

In order to understand the interactions of ZG16p with PIM glycans, saturation-transfer difference (STD)-NMR spectra were recorded (Figure 2). In each case, there was a 100-fold excess of ligand over protein in the NMR buffer (PBS, pH 7.4, 99% D_2O). Under these conditions, PIM1 glycan **1** apparently exhibited a potent STD-NMR signal, whereas glycerol (asterisks in Figure 2A and C), which could not be fully removed during the purification process of ZG16p, nearly disappeared. This clearly



Scheme 2. Synthesis of PIM glycans **1** and **2**. Reagents and conditions: a) PMBCl (1 equiv), NaH, DMF, -20°C , 41% (69% based on recovered starting material); b) BnBr, NaH, DMF, 0°C , 90%; c) CHCl_3/TFA (9:1), 93%; d) **5** (1.3 equiv), TMSOTf, toluene, -40°C , 84%; e) i: $[\text{Ir}(\text{COD})(\text{PPh}_2\text{Me})_2]\text{PF}_6$, H_2 , THF; ii: $\text{HCl}_{(\text{aq})}$, 92%; f) i: **7**, PivCl, pyridine; ii: I_2 , H_2O , 79%; g) NaH, MeOH, 99%; h) 10% Pd/C, H_2 , MeOH, 98%; i) **5** (2.6 equiv), TMSOTf, toluene, -40°C , 62%; j) PdCl_2 , $\text{CH}_2\text{Cl}_2/\text{MeOH}$ (1:1), 64%; k) i: **7**, PivCl, pyridine; ii: I_2 , H_2O , 68%; l) NaH, MeOH, 78%; m) 10% Pd/C, H_2 , MeOH, 92%.

indicates that the main constituent in the STD-NMR spectrum shown in Figure 2B reflects the saturation transfer effect from ZG16p. Likewise, PIM2 glycan **2** exhibited potent STD-NMR signals, thus confirming binding to ZG16p (Figure 2C and D).

The relative STD effects (STD%) suggest that the most pronounced interactions between PIMs and ZG16p were at protons at C3–C6 of the mannose residue (Figure 2E). In the case of the monomannosylated PIM1 glycan **1**, the binding epitope is mainly the pyranose ring at C3–C6, because the protons showed a potent saturation effect (70–100%), whereas the inositol moiety showed weaker saturation (<70%). Although the data obtained under these conditions must be considered qualitative, this observation is consistent with the crystal structure of ManOMe–ZG16p complex (PDB ID: 3VZF), where C4–C6 of mannose interact with the protein.^[6] In the case of PIM2 glycan **2**, protons at M4 and M'4 exhibited similar saturation effects. Although partial signal overlapping at positions 2, 3, and 5 of two mannoses prevents precise epitope mapping, the data imply that ZG16p interacts with PIM2 at the mannose residues.

TR-NOE analysis of the PIM1 and 2 glycans bound with ZG16p

In order to investigate the interactions of PIM glycans, we collected $^1\text{H},^1\text{H}$ NOESY spectra (Figure 3). In order to minimize spin diffusion, the appropriate mixing time was determined by the NOE build-up curve (Figure S2). The 2D $^1\text{H},^1\text{H}$ NOESY spec-

trum of PIM1 glycan **1** (4.6-fold excess) in the presence of ZG16p provided the key inter-residual correlation between Man-H1 and Ino-H2, and intra-residual correlations in negative NOE (Figure 3A). In contrast, no correlation was observed when using the D151N ZG16p mutant (Figure 3B). These data suggest that the identified NOEs are transferred (TR)-NOEs originating from ZG16p-bound state. The atomic distance of inter-residue Man-H1–Ino-H2 was determined as 2.2 Å from relative intensity of the signal.

The $^1\text{H},^1\text{H}$ NOESY spectrum of PIM2 glycan **2** (4.6-fold excess) with ZG16p provided inter-residual correlations in Man-H1–Ino-H2, Man'-H1–Ino-H6, and Man'-H1–InoH1 in negative NOE (Figure 3C). In contrast, only the trace NOE correlations were identified in the control spectrum (ZG16p-D151N; Figure 3D). The atomic distances of the inter-residue protons, ManH1–InoH2, Man'H1–InoH6, and Man'H1–InoH1, were determined at 2.3, 2.2, and 2.8 Å, respectively. We observed TR-NOE signals, thus also suggesting selective binding of PIMs to ZG16p. The binding site was further analyzed in titration experiments.

Chemical shift perturbation experiments of ZG16p with phosphoglycans PIM1 and PIM2

The interaction site(s) of the ligands on ZG16p was determined by chemical shift perturbation experiments and $^1\text{H},^{15}\text{N}$ HSQC spectra. To achieve this, we prepared uniformly ^{15}N -labeled ZG16p (^{15}N [ZG16p]) for $^1\text{H},^{15}\text{N}$ HSQC, and $^{13}\text{C},^{15}\text{N}$ doubly labeled ZG16p ($^{13}\text{C},^{15}\text{N}$ [ZG16p]) for sequential signal assignments. The

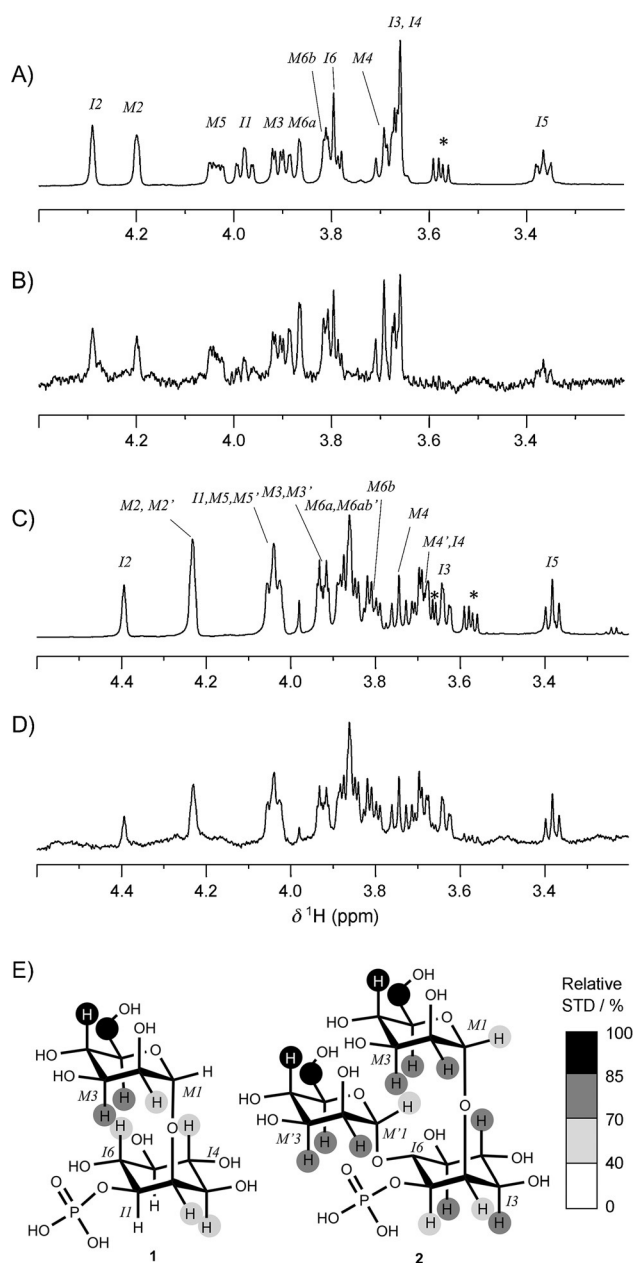


Figure 2. STD-NMR binding epitope of PIM1 glycan 1 and PIM2 glycan 2 to ZG16p: A) ^1H NMR off-resonance spectrum, and B) STD-NMR spectrum of PIM1 glycan 1; C) ^1H NMR off-resonance spectrum, and D) STD-NMR spectrum of PIM2 glycan 2. E) The binding epitopes of PIM1 and PIM2 were determined by relative STD (STD%). In PIM2 glycan 2, STD effects were assigned as identical for overlapping signals at M2/M2', M3/M3', and M5/M5'. Asterisks indicate signals from residual glycerol (in the protein purification buffer). The STD-NMR spectra were collected at 5 °C for samples in PBS (pH 7.4, 99% D_2O). I: inositol, M: mannose

assignment of the backbone amide signals of ZG16p was achieved for $^{13}\text{C},^{15}\text{N}$ ZG16p in 2D and 3D NMR experiments (Table S1).^[29]

PIM1 glycan 1 and PIM2 glycan 2 were titrated into a ^{15}N ZG16p solution, and the signal perturbations were recorded (Figure 4). The results suggest that binding is a fast exchange process, because each set of specific signals featured a gradual chemical-shift change under the titration conditions.

The results of the titration with PIM1 glycan 1 are depicted in Figure S3, and the weighted $^1\text{H},^{15}\text{N}$ chemical-shift changes ($\Delta\delta_{\text{avg}}$) of ZG16p upon addition of a 20-fold excess of 1 are in Figure 5A. The backbone amide signals of Lys36, Arg37, and Gly147 showed large chemical-shift changes ($\Delta\delta_{\text{avg}} > 0.06$), whereas those of Gly35, Ser146, and Leu149 were moderate ($0.04 < \Delta\delta_{\text{avg}} < 0.06$). Small chemical-shift changes ($0.025 < \Delta\delta_{\text{avg}} < 0.04$) were observed for Glu29, Tyr30, Gly31, Ser32, Gly33, Gly34, Arg37, Asp82, Asn129, Ile142, Arg145, Asp151, and Ala152. During the titration, the Leu149 signal broadened at 20-fold ligand excess. In addition, the signal from Arg37 was strongly affected ($\Delta\delta_{\text{avg}}$, 0.06). The K_{D} of PIM1 glycan 1 was 5.0 mM (Figure S4A).

The backbone amide signals perturbed on titration with PIM2 glycan 2 were very similar to those with PIM1 (Figure 5). The $\Delta\delta_{\text{avg}}$ of ^{15}N ZG16p upon addition of a 20-fold excess of 2 (Figure 5B) revealed large chemical-shift changes for Gly35, Lys36, Arg37, and Gly147 ($\Delta\delta_{\text{avg}} > 0.09$). Moderate chemical-shift changes ($0.06 < \Delta\delta_{\text{avg}} < 0.09$) were observed for Gly33, Gly34, Ser146, Asp151, and Ala152, and small changes ($0.03 < \Delta\delta_{\text{avg}} < 0.06$) were seen for Glu29, Tyr30, Gly31, Ser32, Ile142, Val62, Val76, Asp82, and Arg145. The perturbed signals appeared to broaden at an earlier stage in the titration compared with PIM1 glycan 1. For example, the signals for Gly35 and Gly147 were broad in the presence of a 20-fold excess of PIM2 glycan 2, whereas the corresponding signals remained sharp in the presence of a 20-fold excess of PIM1 glycan 1. Additionally, the Leu149 signal broadened before the 20-fold excess of ligand was reached. These results might reflect a chemical exchange process induced by PIM2 glycan 2, similar to the NMR time scale. The titration yielded a K_{D} for PIM2 glycan 2 of 3.0 mM (Figure S4B). The limited differences in perturbed backbone NH signals between PIM1 and PIM2 glycans 1 and 2 support both glycans interacting at the same binding site.

To clarify the interaction between ZG16p and PIMs, the amino acid residues that showed chemical-shift perturbations were identified onto the crystal structure^[5] (Figure 6; heat map color scale reflects the averaged chemical-shift changes in the PIM2 titration). The mapping clearly indicates that most of the perturbed residues are at the surface of the protein, except for Asp82 and Ile142. The ligand-binding site is nearly identical to that for mannose-specific plant lectins of the Jacalin-related lectin family with a Greek-key motif.^[30] They are in two segments, the GG loop (Gly29–Arg37) and the binding loop (Ser146–Ala152). The two loops form a shallow ligand-binding site, with Gly33, Gly34, Gly35, and Gly147 below, Arg37, Arg145, and Lys36 on one side, and Asp151 on the other; these can easily accommodate a mannose residue.

Model of ZG16p-PIM1 complex

Human ZG16p has a higher affinity for PIM1 glycan 1 and PIM2 glycan 2 ($K_{\text{D}} = 5.0$ and 3.0 mM, respectively) than α -methylmannoside (ManOMe, $K_{\text{D}} = 15$ mM, Figure S4C), even though the contact-site epitopes are almost identical. This implies that additional residues (not identified by $^1\text{H},^{15}\text{N}$ HSQC measurements) might be involved in phosphoglycan binding. Attempts to co-

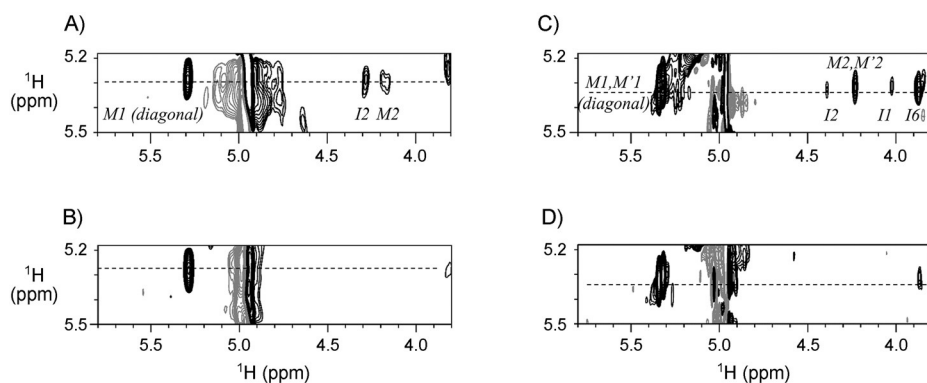


Figure 3. NOESY spectra of A) PIM1 glycan 1 with ZG16p, B) PIM1 glycan 1 with ZG16p-D151N, C) PIM2 glycan 2 with ZG16p, and D) PIM1 glycan 2 with ZG16p-D151N. The spectra were collected with a mixing time of 250 ms at 10 °C. Gray: positive signals; black: negative signal; dotted lines: chemical shifts of Man-H1 (A and B; PIM1), or Man-H1 and Man'-H1 (C and D; PIM2). Residual HDO signals are observed at ~5.0 ppm.

epitope determined by STD-NMR. The PIM1 mannose-binding mode in the model is consistent with the ZG16p–ManOME X-ray crystal structure (Figure S5).^[6] However, importantly, the model suggests that another amino acid residue (Tyr104) in the recognition loop and the side chain of Ser148 in binding loop interact with the inositol moiety. Unfortunately, the NMR signals from Tyr104 and Ser148 were broadened in the ¹H,¹⁵N HSQC spectrum, possibly due to chemical exchange. Although there is no direct evidence for interactions with Tyr104 and

Ser148, it is very likely that these amino acids are responsible for the tighter binding of PIM1 and PIM2 glycans in comparison to ManOME. In line with this, our structural analysis shows that the hydroxy group of Tyr104 exhibits a water-mediated interaction with Man-O-Ser, thereby assisting ligand binding.^[6]

The chemical-shift perturbation experiments for PIM2 glycan 2 suggest that the binding mode is similar to that for PIM1 glycan 1. However, the STD-NMR epitope analysis indicated the contribution of two mannoses. One possible explanation is that PIM2 has two independent binding modes that use the identical binding site on the protein (Figure S6).

Naturally occurring PIMs have a hydrophobic phosphatidyl group at position O1 of inositol; this anchors it to the cell surface of mycobacteria and is crucial for interactions with different mammalian proteins. For example, mouse CD1d, a known receptor of PIMs, has hydrophobic grooves where acyl chains of glycolipids bind.^[32] ZG16p lacks these structural motifs, and evidently binding of this protein involves the sugar and perhaps the phosphate moiety of PIMs.

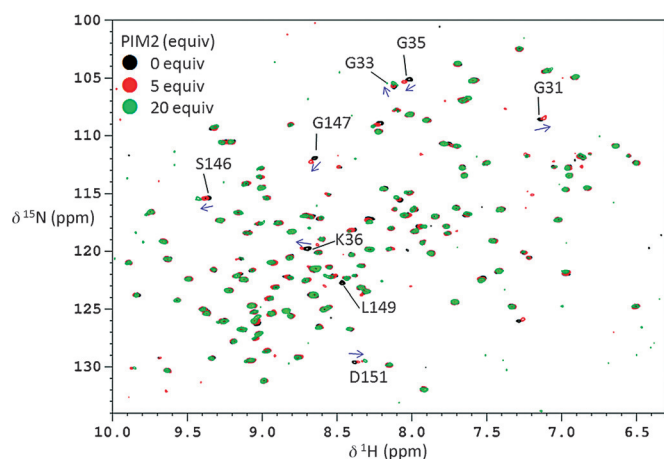


Figure 4. ¹H,¹⁵N HSQC spectra of uniformly ¹⁵N-labeled ZG16p in titration with PIM2 glycan 2. Black: signals with no ligand; red: signals in the presence of 5 equiv of 2; green: signals in the presence of 20 equiv of 2; blue arrows: directions of the chemical-shift changes.

crystallize ZG16p with either PIM1 glycan 1 or PIM2 glycan 2 were unsuccessful. Therefore a PIM–ZG16p complex model based on the crystal structure of glycerol–ZG16p (PDB ID: 3APA)^[5] was constructed. The docking simulation was performed with the Glide^[31] program of the software package Maestro. The resulting models were ranked based on the data obtained by STD and chemical shift perturbation experiments, and a feasible model was thus identified (Figure 7). This was validated by the results from the TR-NOE experiments. The distance between H1 of PIM1 mannose to InoH2 was 2.2 Å in the TR-NOE experiments, and 2.3 Å in the docking simulations.

In the model, the interaction of PIM1 mannose with ZG16p is mediated by intermolecular hydrogen bonds to the backbones of Gly35, Gly147, Ser148, and Leu149, and to the side chain of Asp151 (GG loop and binding loop; Figure 7). In PIM1, hydroxy groups at mannose positions 4 and 6 are highly involved in the hydrogen bonds. This is consistent with our chemical shift perturbation experiments and with the binding

Conclusion

We demonstrate that ZG16p preferentially interacts with *Mycobacterium* glycolipids PIM1 and PIM2 over PIM6 and other mycobacterial glyco-components. STD-NMR studies reveal the interaction of this human lectin with the C3–C6 moiety of the mannose residue. NMR perturbation experiments demonstrate that the phosphoglycans of PIMs interact with the GG loop (Gly31–Lys36) and the binding loop (Ser146–Asp151) of ZG16p, and that their dissociation constants are three to five-fold lower than those of ManOME. Docking simulations combined with NMR data implicate Tyr104 (in the recognition loop) in an interaction with the inositol moiety of the PIMs. ZG16p might play a role in the mucosal immune response by associating with exogenous short PIMs of pathogenic bacteria, including *M. tuberculosis*, and with endogenous glycosaminoglycans at independent binding sites. Further work is required to elucidate the physiological function of this lectin.

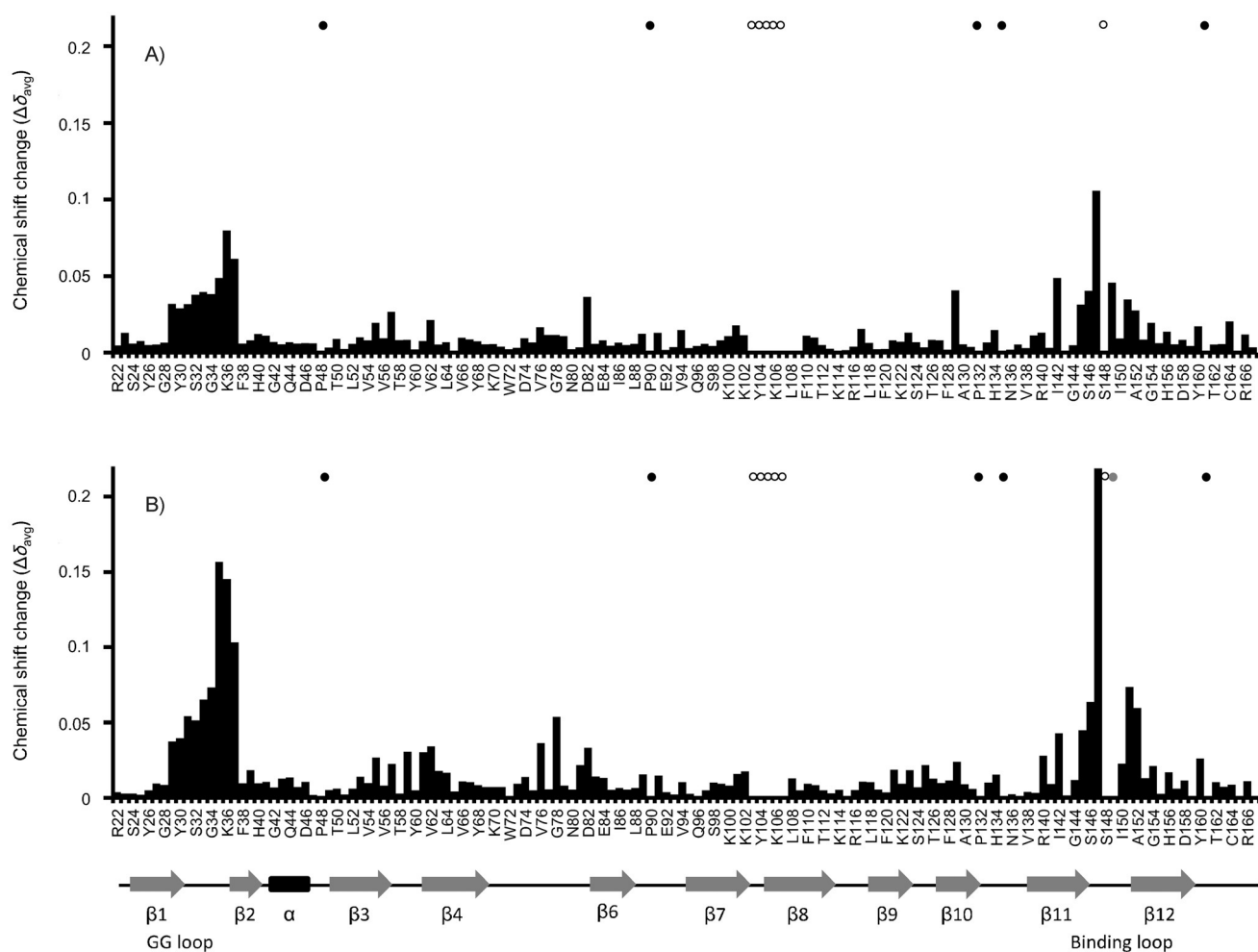


Figure 5. The weighted $^1\text{H},^{15}\text{N}$ chemical-shift changes ($\Delta\delta_{\text{avg}}$) of the backbone amide of ^{15}N ZG16p upon binding with a 20-fold excess of A) PIM1 glycan 1 or B) PIM2 glycan 2. ●: proline; ○: undetermined signals; ●: signal could not be analyzed because of perturbation effects.

Experimental Section

Expression and preparation of ZG16p: Recombinant ZG16p protein, uniformly ^{15}N -labeled (^{15}N ZG16p), and uniformly $^{13}\text{C}/^{15}\text{N}$ -labeled ($^{13}\text{C},^{15}\text{N}$ ZG16p) were prepared in the pCold-MBP (maltose-binding protein) vector, according to a previously reported procedure with slight modifications.^[5] DNA fragments encoding human ZG16p (residues 21–159 for crystallization, 21–167 for NMR; the core lectin domain) were subcloned into pCold-MBP^[35] for the production of recombinant proteins. For the microarray analysis, glutathione-S-transferase (GST)-tagged ZG16p protein (21–167) and its mutant GST-ZG16p-D151N were prepared in the pCold-GST vector, which was modified from pCold vector (Takara Bio Inc., Japan). The plasmid constructs were transformed into *Escherichia coli* BL21(DE3) codon plus (Stratagene), and the cells were grown at 37 °C in either LB medium, M9 with ^{15}N NH₄Cl (ISOTEC, Kürten-Herweg, Germany; for ^{15}N ZG16p), or Spectra 9 (Cambridge Isotope Laboratories, Tewksbury, MA; for $^{13}\text{C},^{15}\text{N}$ ZG16p). After induction with isopropyl β -D-thiogalactoside (0.1 mM), the cells were cultured at 15 °C for 24 h, then harvested, resuspended, and sonicated in Tris-HCl (50 mM, pH 8.0) containing NaCl (50 mM), and Bugbuster (Novagen/Merck Millipore). After centrifugation, the supernatants containing His₆-MBP-fused protein was collected and applied to a Ni Sepharose column (GE Healthcare) equilibrated with PBS (Na₂HPO₄ (8 mM, pH 7.4), KH₂PO₄ (1 mM), NaCl (137 mM),

KCl (3 mM)). After washing with PBS, the protein was eluted in PBS containing imidazole (500 mM). The His₆-MBP tag was removed by digestion with TEV protease at 4 °C for 12 h. The digested proteins were passed through a Ni-Sepharose column, and final purification was performed by size-exclusion chromatography (HiLoad 16/60 Superdex 75 pg; GE Healthcare) or cation exchange chromatography (TOYOPEARL SP-650M or Giga Cap S-650M; Tosoh, Tokyo, Japan). The buffer of the purified proteins were replaced with PBS including D₂O (99 or 10%, v/v); the pH was adjusted to 7.4 for ligand experiments by STD-NMR and TR-NOESY, and to pH 6.5 for $^1\text{H},^{15}\text{N}$ HSQC and backbone amide focusing experiments.

Glycan microarray analysis: The microarrays comprised four manose-containing neoglycolipids (NGLs), nine mycobacterial compounds for antigen preparations (Biodefense and Emerging Infections Research Resources Repository; <http://www.beiresources.org/>), and three fungal-derived glucan polysaccharides (sample information in Table 1). The arrays were generated robotically using a non-contact arrayer on nitrocellulose coated microarray slides.^[17e] All the probes were arrayed with carrier lipids (phosphatidylcholine and cholesterol; Sigma-Aldrich) as previously described,^[17e] except for *M. tuberculosis* arabinogalactan and the glucan polysaccharides (positions 17–20); these were arrayed without lipid carriers. The lipid-linked probes (positions 1–8) were arrayed at 2 and 5 fmol per spot, and these samples were quantified based on primulin

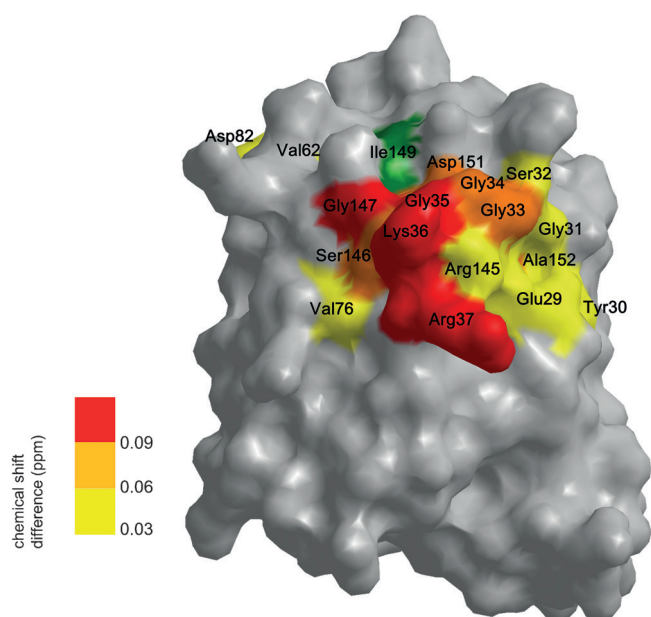


Figure 6. Mapping surface residues in the PIM2 glycan interaction on the crystal structure of human ZG16p (PDB ID; 3APA).^[5] Ile142 (shift $\Delta\delta_{\text{avg}}$ 0.04) is inside the protein. The signal from Ile149 (green) was broadened upon PIM2 binding.

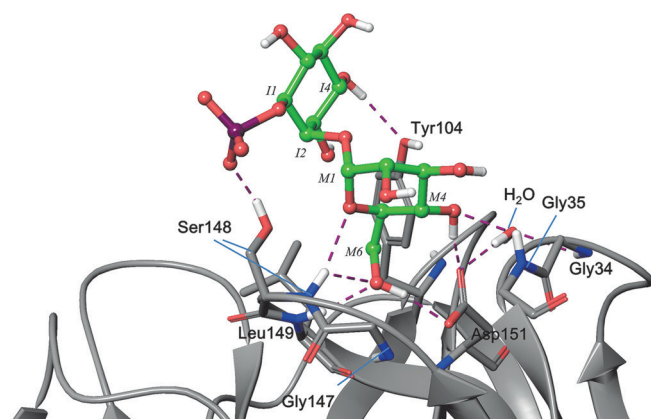


Figure 7. Binding model of PIM1 glycan to human ZG16p, created with docking simulations. The purple dot lines indicate potential hydrogen bond (3.0 Å).

staining of lipid tags.^[17e] The bacterial-and fungal-derived glycoconjugates and polysaccharides (positions 9–20) were arrayed at 0.03 and 0.1 ng per spot (dry weight of the samples received from commercial sources; see Table 1). Microarray analysis with GST-tagged ZG16p (GST-ZG16p and GST-ZG16p-D151N) were performed as described previously.^[17e,36] In brief, microarray slides were blocked at room temperature for 60 min with bovine serum albumin (BSA; 3% (w/v) in PBS). GST-ZG16p and GST-ZG16p-D151N were overlaid (100 $\mu\text{g mL}^{-1}$ as neat, supplemented with 1% BSA) and incubated for 90 min, followed by rabbit anti-GST antibody Z-5 (1:200; Santa Cruz Biotechnology), and then biotinylated anti-rabbit IgG (1:200; Sigma–Aldrich). Biotinylated concanavalin A (Con A; Vector Laboratories, Peterborough, UK) was analyzed at 0.5 and 15 $\mu\text{g mL}^{-1}$. Binding was detected with Alexa Fluor-647-labeled streptavidin (1 $\mu\text{g mL}^{-1}$; Molecular Probes/Life Technologies).

Chemical synthesis of PIM1 and PIM2 glycans: Synthesis and NMR spectra are in the Supporting Information.

General procedures for NMR experiments: NMR spectra were recorded with 500, 600, 700, and 800 MHz spectrometers (Bruker). Protein solutions in PBS (sodium phosphate (10 mM, pH 6.5 or 7.4) with NaCl (150 mM); in 99 or 10% (v/v) D_2O) were used for NMR experiments. ^1H NMR chemical shifts were calibrated with an exterior standard chemical shift (4,4-dimethyl-4-silapentane-1-sulfonic acid (DSS), set to 0 ppm). ^{13}C and ^{15}N chemical shifts were calibrated by indirect referencing based on IUPAC-IUB recommended X/ ^1H resonance ratios (0.251449530 ($^{13}\text{C}/^1\text{H}$); 0.10132911 ($^{15}\text{N}/^1\text{H}$)).^[37] NMR data were processed with XWIN-NMR (ver. 3.5, Bruker) and TopSpin (ver. 3.1, Bruker). The spectra were analyzed with SPARKY 3 (T. D. Goddard and D. G. Kneller, University of California, San Francisco) and displayed with XWIN-PLOT (ver. 3.5, Bruker).

STD-NMR: 1D STD-NMR experiments were performed in a 600 MHz spectrometer with a TXI probe. The protein signal at -0.5 or -1 ppm was saturated with a 50 ms Gaussian pulse train with 60 times (on-resonance); reference spectra were obtained with irradiation at 40 ppm (off-resonance). The on-resonance and off-resonance spectra were collected in an interleaved manner, and accumulated into two different data sets. Water suppression was achieved with a WATERGATE pulse sequence (3–9–19 pulse train). In STD-NMR experiments, 64 scans with three repetition loops were required to obtain a good signal-to-noise ratio, and protein signals were partially suppressed by using a 3–10 ms spin-lock pulse. In binding epitope analyses, the signal intensities were evaluated from $(I_{\text{off}} - I_{\text{on}})/I_{\text{off}}$, where I_{on} is the on-resonance signal intensity and I_{off} is off-resonance signal intensity. The values were normalized within each glycan structure (highest value assigned 100%). Unlabeled ZG16p (50 μM) in PBS (pH 7.4, 99% D_2O) was used for STD-NMR experiments, and 100-fold excess of ligand (PIM1 glycan 1 or PIM2 glycan 2) was titrated into the protein solution.

TR-NOESY: 2D $^1\text{H},^1\text{H}$ NOESY spectra were collected in a 700 MHz spectrometer equipped with TCI probe (probe temperature, 10 $^\circ\text{C}$). The residual HDO signal was suppressed by using WATERGATE pulse sequence with a 3–9–19 pulse train. NOESY spectra of PIM1 glycan 1 (300 μM) in PBS (500 μL , 99% D_2O , pH 7.4) were collected in the presence of ZG16p (65 μM) or ZG16p-D151N (60 μM). The data were collected as 1024 (F2) \times 256 (F1) data points with 32 scans (mixing times: 150, 250, 350, 500, and 700 ms). NOESY spectra for PIM2 glycan 2 (300 μM) in PBS (250 μL , 99% D_2O , pH 7.4) were collected in the presence of ZG16p (65 μM) or ZG16p-D151N (60 μM) by using micro-cells (Shigemi, Tokyo, Japan). The data were collected as 2048 (F2) \times 256 (F1) data points (32 or 64 scans; mixing times, 150, 250, 350, and 500 ms).

$^1\text{H},^{15}\text{N}$ HSQC titration experiment: $^1\text{H},^{15}\text{N}$ HSQC spectra were obtained in a 500 MHz spectrometer equipped with a cryo-TXI probe (probe temperature 25 $^\circ\text{C}$). The spectra were collected with 1024 (F2) \times 256 (F1) data matrix points with either four or eight scans. Appropriate molar equivalents of PIM1 glycan 1 or PIM2 glycan 2 (20 mM in PBS with 10% D_2O , pH 6.5) were added to [^{15}N]ZG16p (0.1 mM) in PBS (pH 6.5, 10% D_2O), and submitted to $^1\text{H},^{15}\text{N}$ HSQC analysis. Weighted averages of ^1H and ^{15}N chemical-shift changes ($\Delta\delta_{\text{avg}}$) were calculated from Equation (1):

$$\Delta\delta_{\text{avg}} = [(\Delta\delta_{\text{H}})^2 + (0.2 \times \Delta\delta_{\text{N}})^2]^{1/2} \quad (1)$$

where $\Delta\delta_{\text{H}}$ and $\Delta\delta_{\text{N}}$ are the observed chemical-shift changes (ppm) of ^1H and ^{15}N . The backbone amide signals of [$^{13}\text{C},^{15}\text{N}$]ZG16p (0.2 mM) were assigned sequentially via analysis of 3D HNCA, HN(CO)CA, HNCACB, and CBCA(CO)NH spectra obtained from an

800 MHz spectrometer equipped with a cryo-TCL probe at 25 °C (Table S1).

Modeling of PIM1-ZG16p complex: The docking of PIM1 glycan 1 to ZG16p was performed in the software package Glide 5.8^[31] of the Maestro suite (ver. 9.3.5, Schrödinger, LLC, New York). Prior to docking, ZG16p (PDB ID; 3APA^[5]) was prepared using Protein Preparation Wizard by adding hydrogen, assigning bond orders, and optimizing bond lengths, bond angles, and torsion angles. The minimization was performed with the force field OPLS-2005. The ligand glycan was prepared with LigPrep and minimized using the force field OPLS-2005. The receptor glide was generated based on the glycerol in the crystal data. The docking study was performed using a standard precision (SP) Glide docking with default parameters. For PIM1 glycan 1, several ligand poses were provided, and the model with the highest docking score (−4.0) agreed best with the NMR data. All possible ligand poses were manually evaluated based on the STD-NMR data and the ¹H,¹⁵N HSQC titration results.

Acknowledgements

This work was supported in part by funding from RIKEN-Max Planck Joint Research Center, the UK Research Council Basic Technology Initiative Glycoarrays (GRS/79268) and Translational Grant (EP/G037604/1), the Wellcome Trust biomedical resource grants WT093378MA and WT099197MA (T.F.), Grant-in-Aid for Young Scientists (B) (24710257) and for Scientific Research (C) (25460054) from the Japan Society for the Promotion of Science (S.H., Y.Y.), and by a SUNBOR GRANT from the Suntory Foundation of Life Sciences (S.H.). We acknowledge BEI Resources (NIAID, NIH) for the Mycobacterial glycoconjugates. We thank members of the Glycosciences Laboratory for their collaboration in the establishment of the neoglycolipid-based microarray system. We thank Dr. Yutaka Muto (RIKEN Yokohama) for his help in acquiring and processing 3D NMR data. We thank Dr. Yukishige Ito (RIKEN, ERATO) and Prof. Osamu Kanie (ERATO, Tokai University) for enabling us to use the cryoprobe-equipped NMR spectrometer. We thank Dr. Mayumi Kanagawa (RIKEN) for her efforts in trying to co-crystallize ZG16p and PIMs. We acknowledge Masaki Kato (RIKEN) and RIKEN Integrated Cluster of Clusters (RICC) facility for the trial of MD simulations. We thank Noriko Tanaka (RIKEN) for secretarial assistance and Dr. Yu-Hsuan Tsai and Dr. Ivan Vilotijevic for valuable discussions regarding the synthesis of PIM1 and 2. We thank Drs. Iria Uhia and Brian D. Robertson (Imperial College London) for specialist opinions on ZG16p-mycobacteria interactions.

Keywords: carbohydrate microarrays • chemical synthesis • lectins • microarrays • NMR spectroscopy • phosphatidyl inositol mannoside

- [1] U. Cronshagen, P. Volland, H. F. Kern, *Eur. J. Cell Biol.* **1994**, *65*, 366–377.
- [2] H. Tateno, R. Yabe, T. Sato, A. Shibazaki, T. Shikanai, T. Gono, H. Narimatsu, J. Hirabayashi, *Glycobiology* **2012**, *22*, 210–220.
- [3] R. Kleene, H. Dartsch, H.-F. Kern, *Eur. J. Cell Biol.* **1999**, *78*, 79–90.
- [4] K. Kumazawa-Inoue, T. Mimura, S. Hosokawa-Tamiya, Y. Nakano, N. Dohmae, A. Kinoshita-Toyoda, H. Toyoda, K. Kojima-Aikawa, *Glycobiology* **2012**, *22*, 258–266.

- [5] M. Kanagawa, T. Satoh, A. Ikeda, Y. Nakano, H. Yagi, K. Kato, K. Kojima-Aikawa, Y. Yamaguchi, *Biochem. Biophys. Res. Commun.* **2011**, *404*, 201–205.
- [6] M. Kanagawa, Y. Liu, S. Hanashima, A. Ikeda, W. Chai, Y. Nakano, K. Kojima-Aikawa, T. Feizi, Y. Yamaguchi, *J. Biol. Chem.* **2014**, *289*, 16954–16965.
- [7] a) K. Drickamer, *Curr. Opin. Struct. Biol.* **1999**, *9*, 585–590; b) C. G. Figdor, Y. van Kooyk, G. J. Adema, *Nat. Rev. Immunol.* **2002**, *2*, 77–84; c) T. B. H. Geijtenbeek, S. I. Gringhuis, *Nat. Rev. Immunol.* **2009**, *9*, 465–479.
- [8] a) C. A. Wells, J. A. Salvage-Jones, X. Li, K. Hitchens, S. Butcher, R. Z. Murray, A. G. Beckhouse, Y.-L. S. Lo, S. Manzanero, C. Cobbold, K. Schroder, B. Ma, S. Orr, L. Stewart, D. Lebus, P. Sobieszczuk, D. A. Hume, J. Stow, H. Blanchard, R. B. Ashman, *J. Immunol.* **2008**, *180*, 7404–7413; b) S. Yamasaki, M. Matsumoto, O. Takeuchi, T. Matsuzawa, E. Ishikawa, M. Sakuma, H. Tateno, J. Uno, J. Hirabayashi, Y. Mikami, K. Takeda, S. Akira, T. Saito, *Proc. Natl. Acad. Sci. USA* **2009**, *106*, 1897–1902; c) E. Ishikawa, T. Ishikawa, Y. S. Morita, K. Toyonaga, H. Yamada, O. Takeuchi, T. Kinoshita, S. Akira, Y. Yoshikai, S. Yamasaki, *J. Exp. Med.* **2009**, *206*, 2879–2888.
- [9] L. de Witte, A. Nabatov, M. Pion, D. Fluitsma, M. A. W. P. de Jong, T. de Gruijl, V. Piguët, Y. van Kooyk, T. B. Geijtenbeek, *Nat. Med.* **2007**, *13*, 367–371.
- [10] a) H. Tateno, K. Ohnishi, R. Yabe, N. Hayatsu, T. Sato, M. Takeya, H. Narimatsu, J. Hirabayashi, *J. Biol. Chem.* **2010**, *285*, 6390–6400; b) H. Feinberg, M. E. Taylor, N. Razi, R. McBride, Y. A. Knirel, S. A. Graham, K. Drickamer, W. I. Weis, *J. Mol. Biol.* **2011**, *405*, 1027–1039.
- [11] a) R. A. Childs, K. Drickamer, T. Kawasaki, S. Thiel, T. Mizuochi, T. Feizi, *Biochem. J.* **1989**, *262*, 131–138; b) K. Takahashi, R. A. B. Ezekowitz, *Clin. Infect. Dis.* **2005**, *41*, S440–S444.
- [12] E. Laurine, X. Manival, C. Montgelard, C. Bideau, J.-L. Bergé-Lefranc, M. Énard, J.-M. Verdier, *Biochim. Biophys. Acta Gene Struct. Expression* **2005**, *1727*, 177–187.
- [13] a) H. L. Cash, C. V. Whitham, C. L. Behrendt, L. V. Hooper, *Science* **2006**, *313*, 1126–1130; b) R. E. Lehotzky, C. L. Partch, S. Mukherjee, H. L. Cash, W. E. Goldman, K. H. Gardner, L. V. Hooper, *Proc. Natl. Acad. Sci. USA* **2010**, *107*, 7722–7727.
- [14] J. Iovanna, J. M. Frigerio, N. Duseti, F. Ramare, P. Raibaud, J. C. Dagorn, *Pancreas* **1993**, *8*, 597–601.
- [15] M.-R. Ho, Y.-C. Lou, S.-Y. Wei, S.-C. Luo, W.-C. Lin, P.-C. Lyu, C. Chen, *J. Mol. Biol.* **2010**, *402*, 682–695.
- [16] a) M. E. Guerin, J. Korduláková, P. M. Alzari, P. J. Brennan, M. Jackson, *J. Biol. Chem.* **2010**, *285*, 33577–33583; b) A. K. Mishra, N. N. Driessen, B. J. Appelmelk, G. S. Besra, *FEMS Microbiol. Rev.* **2011**, *35*, 1126–1157.
- [17] a) T. Feizi, F. Fazio, W. Chai, C.-H. Wong, *Curr. Opin. Struct. Biol.* **2003**, *13*, 637–645; b) J. L. de Paz, T. Horlacher, P. H. Seeberger, *Methods Enzymol.* **2006**, *415*, 269–292; c) I. Shin, S. Park, M.-r. Lee, *Chem. Eur. J.* **2005**, *11*, 2894–2901; d) Y. Liu, T. Feizi, M. A. Campanero-Rhodes, R. A. Childs, Y. Zhang, B. Mulloy, P. G. Evans, H. M. I. Osborn, D. Otto, P. R. Crocker, W. Chai, *Chem. Biol.* **2007**, *14*, 847–859; e) Y. Liu, R. A. Childs, A. S. Palma, M. A. Campanero-Rhodes, M. S. Stoll, W. Chai, T. Feizi, *Methods Mol. Biol.* **2012**, *808*, 117–136.
- [18] M. Gilleron, V. F. J. Quesniaux, G. Puzo, *J. Biol. Chem.* **2003**, *278*, 29880–29889.
- [19] N. N. Driessen, R. Ummels, J. J. Maaskant, S. S. Gurcha, G. S. Besra, G. D. Ainge, D. S. Larsen, G. F. Painter, C. M. J. E. Vandenbroucke-Grauls, J. Geurtsen, B. J. Appelmelk, *Infect. Immun.* **2009**, *77*, 4538–4547.
- [20] S. Boonyarattanakalin, X. Liu, M. Michieletti, B. Lepenies, P. H. Seeberger, *J. Am. Chem. Soc.* **2008**, *130*, 16791–16799.
- [21] a) P. S. Patil, S.-C. Hung, *Chem. Eur. J.* **2009**, *15*, 1091–1094; b) A. Ali, M. R. Wenk, M. J. Lear, *Tetrahedron Lett.* **2009**, *50*, 5664–5666; c) B. S. Dyer, J. D. Jones, G. D. Ainge, M. Denis, D. S. Larsen, G. F. Painter, *J. Org. Chem.* **2007**, *72*, 3282–3288; d) G. D. Ainge, J. Hudson, D. S. Larsen, G. F. Painter, G. S. Gill, J. L. Harper, *Bioorg. Med. Chem.* **2006**, *14*, 5632–5642; e) A. Stadelmaier, R. R. Schmidt, *Carbohydr. Res.* **2003**, *338*, 2557–2569; f) C. J. J. Elie, C. E. Dreef, R. Verduyn, G. A. Van Der Marel, J. H. Van Boom, *Tetrahedron* **1989**, *45*, 3477–3486.
- [22] X. Liu, B. L. Stocker, P. H. Seeberger, *J. Am. Chem. Soc.* **2006**, *128*, 3638–3648.
- [23] A. Ravidà, X. Liu, L. Kovacs, P. H. Seeberger, *Org. Lett.* **2006**, *8*, 1815–1818.

- [24] J. J. Oltvoort, C. A. A. Van Boeckel, J. H. De Koning, J. H. Van Boom, *Synthesis* **1981**, 305–308.
- [25] L. Knerr, X. Pannecoucke, G. Schmitt, B. Luu, *Tetrahedron Lett.* **1996**, *37*, 5123–5126.
- [26] a) M. Mayer, B. Meyer, *J. Am. Chem. Soc.* **2001**, *123*, 6108–6117; b) M. Mayer, B. Meyer, *Angew. Chem. Int. Ed.* **1999**, *38*, 1784–1788; *Angew. Chem.* **1999**, *111*, 1902–1906; c) B. Meyer, T. Peters, *Angew. Chem. Int. Ed.* **2003**, *42*, 864–890; *Angew. Chem.* **2003**, *115*, 890–918.
- [27] a) C. A. Lepre, J. M. Moore, J. W. Peng, *Chem. Rev.* **2004**, *104*, 3641–3676; b) A. Ardá, P. Blasco, D. Varón Silva, V. Schubert, S. André, M. Bruix, F. J. Cañada, H.-J. Gabius, C. Unverzagt, J. Jiménez-Barbero, *J. Am. Chem. Soc.* **2013**, *135*, 2667–2675.
- [28] C. P. J. Glaudemans, L. Lerner, G. D. Daves, Jr., P. Kovac, R. Venable, A. Bax, *Biochemistry* **1990**, *29*, 10906–10911.
- [29] A. S. Edison, F. Abildgaard, W. M. Westler, E. S. Mooberry, J. L. Markley, *Methods Enzymol.* **1994**, *239*, 3–79.
- [30] a) Y. Bourne, V. Zamboni, A. Barre, W. J. Peumans, E. J. M. Van Damme, P. Rougé, *Structure* **1999**, *7*, 1473–1482; b) Y. Bourne, V. Roig-Zamboni, A. Barre, W. J. Peumans, C. H. Astoul, E. J. M. Van Damme, P. Rougé, *J. Biol. Chem.* **2004**, *279*, 527–533.
- [31] R. A. Friesner, J. L. Banks, R. B. Murphy, T. A. Halgren, J. J. Klicic, D. T. Mainz, M. P. Repasky, E. H. Knoll, M. Shelley, J. K. Perry, D. E. Shaw, P. Francis, P. S. Shenkin, *J. Med. Chem.* **2004**, *47*, 1739–1749.
- [32] D. M. Zajonc, G. D. Ainge, G. F. Painter, W. B. Severn, I. A. Wilson, *J. Immunol.* **2006**, *177*, 4577–4583.
- [33] K. Schmidt, M. Schrader, H.-F. Kern, R. Kleene, *J. Biol. Chem.* **2001**, *276*, 14315–14323.
- [34] K. Hase, K. Kawano, T. Nochi, G. S. Pontes, S. Fukuda, M. Ebisawa, K. Kadokura, T. Tobe, Y. Fujimura, S. Kawano, A. Yabashi, S. Waguri, G. Nakato, S. Kimura, T. Murakami, M. Imura, K. Hamura, S.-I. Fukuoka, A. W. Lowe, K. Itoh, H. Kiyono, H. Ohno, *Nature* **2009**, *462*, 226–230.
- [35] a) T. Satoh, Y. Chen, D. Hu, S. Hanashima, K. Yamamoto, Y. Yamaguchi, *Mol. Cell* **2010**, *40*, 905–916; b) K. Hayashi, C. Kojima, *J. Biomol. NMR* **2010**, *48*, 147–155.
- [36] A. S. Palma, T. Feizi, Y. Zhang, M. S. Stoll, A. M. Lawson, E. Díaz-Rodríguez, M. A. Campanero-Rhodes, J. Costa, S. Gordon, G. D. Brown, W. Chai, *J. Biol. Chem.* **2006**, *281*, 5771–5779.
- [37] D. S. Wishart, C. G. Bigam, J. Yao, F. Abildgaard, H. J. Dyson, E. Oldfield, J. L. Markley, B. D. Sykes, *J. Biomol. NMR* **1995**, *6*, 135–140.

 Manuscript received: March 13, 2015

Accepted article published: April 28, 2015

Final article published: June 11, 2015